

# Reactions of lead cluster ions with acetone

Zhixin Tian<sup>†</sup>, Xiaopeng Xing<sup>†</sup> and Zichao Tang<sup>\*</sup>

State Key Laboratory of Molecular Reaction Dynamics, Center of Molecular Science, Institute of Chemistry, Chinese Academy of Sciences, Beijing 100080, People's Republic of China

Received 31 August 2002; Revised 20 October 2002; Accepted 21 October 2002

Reactions of lead cluster cations and anions with acetone have been studied using a homemade reflectron time-of-flight mass spectrometer. Association with acetone to form  $\text{Pb}_k(\text{CH}_3\text{COCH}_3)_n^+$ , high-energy pathway reactions forming  $\text{Pb}_k\text{CH}_3^+$ , and intraheterocluster reaction of  $\text{Pb}_k(\text{CH}_3\text{COCH}_3)_{n+1}^+$  to give  $\text{Pb}_k\text{CH}_3(\text{CH}_3\text{COCH}_3)_n^+$  were the main reaction pathways for lead cluster cations with acetone. Decomposition of acetone by  $\text{Pb}_k^-$  to give  $\text{Pb}_k\text{C}_m^-$  ions and their further association with acetone,  $\text{Pb}_k\text{C}_m(\text{CH}_3\text{COCH}_3)^-$ , were the dominant reactions of lead cluster anions with acetone.  $\text{Pb}_7^-$ ,  $\text{Pb}_{10}^-$ , and  $\text{Pb}_k\text{C}_5^-$  were 'magic numbers' with special structural stability in  $\text{Pb}_k^-$  and  $\text{Pb}_k\text{C}_m^-$ , respectively. In addition,  $\text{Pb}_k\text{H}^-$ ,  $\text{CH}_2\text{COCH}_3(\text{CH}_3\text{COCH}_3)_n^-$  and  $\text{Pb}_k\text{CH}_2\text{COCH}_3(\text{CH}_3\text{COCH}_3)_n^-$  were also observed in the reaction of lead cluster anions. Some reaction mechanisms are proposed for these reactions. To investigate the isotope effect for the reaction of lead cluster cations and anions with acetone and to verify the structural assignments of the observed ions, reactions of lead cluster cations and anions with deuterated acetone- $d_6$  were also performed. Copyright © 2002 John Wiley & Sons, Ltd.

Studies of gas-phase ion/solvent clusters provide a unique and accessible way to investigate the influence of solvation on chemical reaction dynamics within the capacity of presently existing experimental techniques. As a very commonly used solvent, acetone has been widely studied in ion-molecule reactions.<sup>1–6</sup> Selective ion solvation of  $\text{Na}^+$ ,  $\text{Cs}^+$  ions in the mixed solvents of methanol and acetone was studied using vibrational predissociation spectroscopy and infrared spectroscopy.<sup>7,8</sup> Besides main-group metal atomic ions, reactions of acetone with all kinds of transition-metal atomic ions have also been intensively studied. The reactions of  $\text{Fe}^+$ ,  $\text{Co}^+$  with acetone studied by ICR and KERD experiments<sup>9–11</sup> followed the low-energy reaction pathway<sup>10–14</sup> and mainly gave  $\text{CH}_3\text{-CH}_3$  and  $\text{MCO}^+$  as products (with 7% of  $\text{M}(\text{CH}_3)_2^+$  and  $\text{CO}$ ); the same results were obtained with deuterated acetone- $d_6$ . In this low-energy pathway reaction mechanism, besides oxidative insertion of the metal ion into one bond of the ligand molecule, migration of one or more atom (or group) of the ligand molecule then occurs before reductive elimination of a small molecule takes place. Products from the reaction of  $\text{Cu}^+$  with acetone were  $\text{CuCH}_3$  and  $\text{CH}_3\text{CO}^+$ , which were thought to arise from the high-energy reaction pathway<sup>15</sup> (oxidative insertion and then simple bond cleavage are the dominant reaction processes, which often have a favorable frequency factor in

this pathway<sup>15</sup>). Soft acid-soft base interaction was adopted<sup>10</sup> to explain the affinity of  $\text{Cu}^+$  with  $\text{CH}_3^-$ .

In both high- and low-energy reaction pathways, the ionic product with lower ionization potential dominates the dissociation process, in accord with Stevenson's rule.<sup>16</sup> Completely different products ( $\text{MO}^+$  and  $\text{C}_3\text{H}_6$ ) appeared for the reactions of  $\text{Sc}^+$ ,  $\text{Ti}^+$ ,  $\text{Gd}^+$ , and  $\text{Pr}^+$  with acetone in ion-beam studies, for which the mechanism was thought to involve approach of the oxyphilic metal ion first to the oxygen atom.<sup>17–19</sup>

Study of the properties and reactions of lead compounds may contribute to its industrial application.<sup>20–22</sup> Castleman *et al.* have reported the clustering reactions of monovalent lead atomic ions with water<sup>23</sup> and benzene,<sup>24</sup> using high-pressure mass spectrometry; thermodynamic properties of hydrated monovalent lead ions in the gas phase were measured. A bimolecular dehydration reaction was observed in the mixed lead/methanol cluster ions,  $\text{Pb}_k(\text{CH}_3\text{OH})_n^+$  ( $n \geq 3$ ).<sup>25</sup>

We have previously reported the reactions of lead cluster cations and anions with ethylene, propene, and *trans*- and *cis*-butene.<sup>26</sup> Association products were observed for the four alkenes; high-energy pathway reactions occurred for propene and butene, and bond selectivity and effects of steric hindrance were evident in the low-energy pathway reactions of *trans*- and *cis*-butene. In the present work, we report the reactions of lead cluster cations and anions with acetone using a reflectron time-of-flight mass spectrometer. Our interest in this system is for four reasons. Firstly, in the reactions of metal clusters with ligand molecules, lead is a main-group metal rather than a transition-group one, and its special electronic structure (many unfilled orbitals) may lead to special metal-ligand interactions. Secondly, the study of metal cluster ions rather than single metal atomic ions in

\*Correspondence to: Z. Tang, State Key Laboratory of Molecular Reaction Dynamics, Center of Molecular Science, Institute of Chemistry, Chinese Academy of Sciences, Beijing 100080, People's Republic of China.

E-mail: Zichao@mrldlab.icas.ac.cn

<sup>†</sup>Graduate student, Graduate Division, Chinese Academy of Sciences.

organometallic reactions will approach more closely the condensed-phase heterogeneous catalytic reactions, and aid the understanding of the related structure-reactivity relationships. Thirdly, exploiting the behavior of lead (cluster ions), which is a very harmful component in the atmosphere, is useful information for the desire to control and finally eliminate pollution by lead. It is of interest in this regard that acetone cluster ions exist in the upper troposphere between 7 and 15 km.<sup>27</sup> Studies of gas-phase metal ion/acetone clusters may contribute to the study of collisional attachment of atmospheric ions to aerosol particles. Finally, interactions between transition metals and unsaturated carbon-carbon bonds were traditionally explained by the Dewar-Chatt-Duncanson donor-acceptor interaction model;<sup>28,29</sup> however, the reactions that occur when unsaturated carbon-carbon bonds are replaced by unsaturated carbon-oxygen bonds are little known.

## EXPERIMENTAL

The laser target was prepared by grinding lead (purity 99%) into a fine powder and pressing it into a tablet 12 mm in diameter and 5 mm in thickness. Acetone (analytically pure) or deuterated acetone-*d*<sub>6</sub> (NMR reagent) was seeded in argon (purity 99.9%) in a vacuum stainless steel bottle (about 1 L) to yield a total stagnation pressure of 4 atm. The volume ratios of acetone and deuterated acetone-*d*<sub>6</sub> in the mixed gas were 5 and 3.75%, respectively. All materials and chemical reagents were obtained commercially in high purity and used as supplied without any further purification. No impurities were observed in the mass spectra of the samples.

Reactions of lead cluster cations and anions with acetone or deuterated acetone-*d*<sub>6</sub> were performed using a homemade reflectron time-of-flight mass spectrometer (RTOFMS), which has been described in detail elsewhere<sup>26</sup> and only a brief description will be given here. The focused second harmonic output of an Nd:YAG laser was used to ablate the lead target. Pulses of a mixture of acetone or deuterated acetone-*d*<sub>6</sub> seeded in argon were injected by a pulsed nozzle, and directed to cross the laser-generated metal ions to form the reaction gas flux. The central point of the crossing region of the acetone beam and the metal ion beam was 10 mm from the pulsed nozzle and 2.5 mm from the surface of the lead target. The reaction gas flow was then temporarily encaged in the 'growth channel' (diameter × length, 3 × 10 mm), where condensation/nucleation results in formation of lead cluster ions and reactions of these ions with acetone or deuterated acetone-*d*<sub>6</sub> occur. Reaction products formed in these processes are cooled by the supersonic expansion through the exit nozzle opening into the vacuum chamber, where a sudden decrease in density and temperature stops further reaction from occurring. It should be noted that this source configuration was specially designed to produce large metal cluster ions; if the laser-ablated metal ions cross the pulsed expansion beam directly in the vacuum chamber, as in the apparatus of Yang,<sup>30</sup> then generally only metal atomic ions are produced. A schematic diagram of the source configuration is shown in Fig. 1. Simulation results with the 3D-hydro programme<sup>31</sup> predict that the pressure in the 'growth channel' could reach 1 atm and the static tempera-

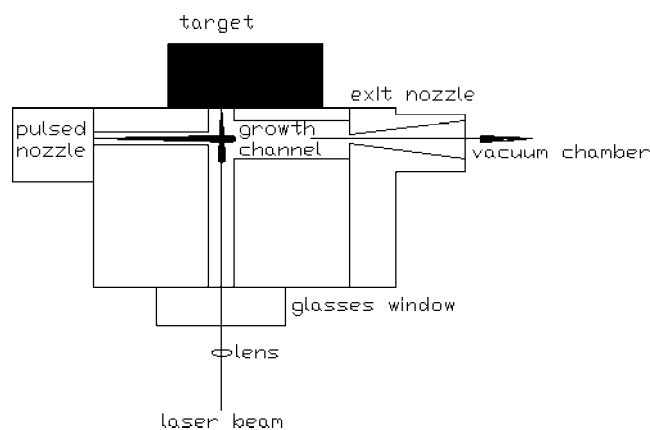


**Figure 1.** Schematic of the experimental setup of the laser vaporization source.

ture is 200–270 K. The axial velocity of the complex in the 'growth channel' is about 100 m/s, which means the reaction time for the reaction gas flow reaches hundreds of microseconds before supersonic expansion. The expansion gas was carried by the pulsed argon through a conical skimmer, and entered the pulsed extraction region of the RTOFMS. The product cations or anions were extracted and detected in the RTOFMS. The timing of valve opening, laser vaporization, pulse acceleration, and recording is optimized in a digital delay pulse generator (Stanford Research DG535). The final digitized TOF mass spectra were typically averaged over 1000 laser pulses to increase the signal-to-noise ratio. To obtain an optimized cluster mass spectrum, adjustments are also made to the duration of the pulsed nozzle, and to the electric fields for extraction, deflection, space focus and reflectron.

The mass resolution of the mass spectrometer for this particular experiment is over 1000 below *m/z* 1000, which enabled the apparatus to resolve hydrogen and deuterium atoms contained in clusters (unit mass resolution), as will be discussed below in the section dealing with lead anions.

## RESULTS AND DISCUSSION

Here we report our experimental results on the reactions of lead cluster cations and anions with acetone. The reaction pathways in the reaction of lead cluster cations included association of acetone to form  $\text{Pb}_k(\text{CH}_3\text{COCH}_3)_n^+$  and a high-energy pathway reaction forming  $\text{Pb}_k\text{CH}_3^+$  and its further association with acetone to give  $\text{Pb}_k\text{CH}_3(\text{CH}_3\text{COCH}_3)_n^+$ . Decomposition of acetone by  $\text{Pb}_k^-$  yielding  $\text{Pb}_k\text{C}_m^-$  and its further association with acetone to give  $\text{Pb}_k\text{C}_m^-(\text{CH}_3\text{COCH}_3)_n^-$  were the main pathways observed for the reaction of lead cluster anions.  $\text{PbH}^-$ ,  $\text{CH}_2\text{COCH}_3^-(\text{CH}_3\text{COCH}_3)_n^-$ ,  $\text{Pb}_k\text{CH}_2\text{COCH}_3(\text{CH}_3\text{COCH}_3)_n^-$  were also observed in the reaction of lead cluster anions with acetone.

### Reactions of lead cluster cations with acetone

Figure 2 shows a typical mass spectrum of cationic products from the reaction of lead cluster cations with acetone.

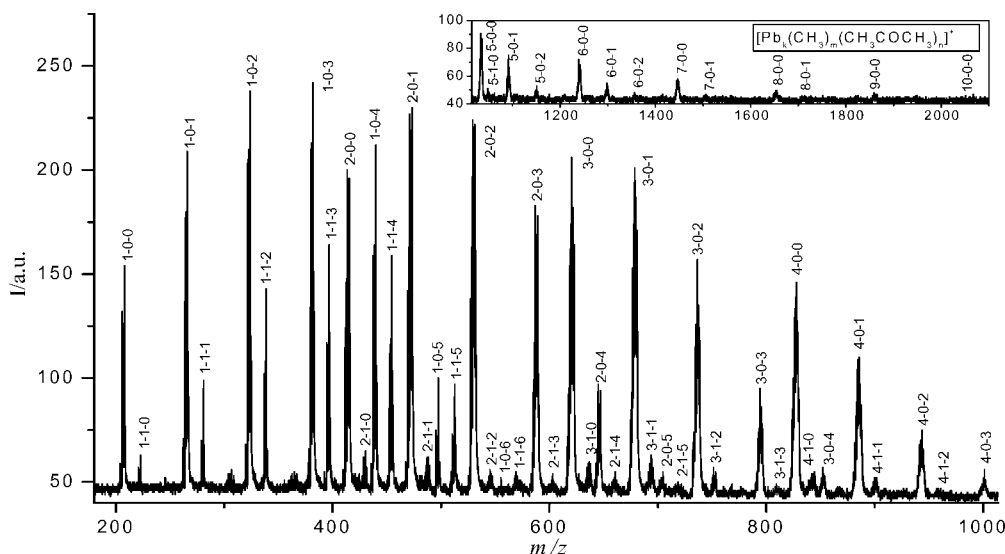


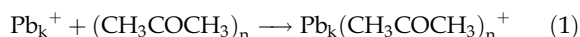
**Figure 2.** Typical TOF mass spectrum for cationic products obtained from the Nd:YAG laser (532 nm, 10 mJ/pulse) irradiation of a lead tablet in the acetone + Ar (95%) mixed carrier gas. The inset (top right) shows the high-mass region.

### $Pb_k^+$ clusters

$Pb_k^+$  ions are among the most abundant cationic species in Fig. 2, and a wide distribution ( $k = 1-10$ ) was observed. No 'magic number' for lead cluster cations  $Pb_k^+$  was observed here, although  $Pb_7^+$  (closed pentagonal bipyramid) and  $Pb_{10}^+$  (capped square antiprism) have been observed as 'magic numbers' elsewhere.<sup>32,33</sup> Seeding of the reaction gas (i.e., acetone) in the carrier gas (Ar) promoted the growth of  $Pb_k^+$  clusters since, when only Ar was used, the intensity of  $Pb_k^+$  clusters was appreciably smaller and indeed  $Pb_k^+$  could usually grow no larger than  $Pb^+$ . This phenomenon was also observed previously for the reactions of lead cluster ions with other small organic molecules such as ethylene, acetylene, ethanol, butene, etc.<sup>26</sup> We believe the underlying mechanism is that the trace organic molecules effectively relax the internal energy (effective temperature) of the laser ablation plasma, which was advantageous for the formation of large-size clusters.

### Association pathway $Pb_k(CH_3COCH_3)_n^+$

Among the predominant cationic species observed in Fig. 2 are the chemisorption species  $Pb_k(CH_3COCH_3)_n^+$  from the association channel, which possibly occurred via reaction (1) in which neutral acetone clusters are 'picked up' by the metal cluster ions formed in the ablation.



The association product ions  $Pb_k(CH_3COCH_3)_n^+$  are probably stabilized by evaporation of one acetone molecule or by collision with the carrier gas (argon). It is known that association products form easily at low collision energies and under multiple-collision conditions.<sup>34</sup> Low-energy collisions are favored in the present source configuration with the lead ion perpendicularly crossing the acetone cluster beam, which faces the extraction region of the mass

spectrometer.<sup>35</sup> The reason why reaction (1) is believed to not be a physisorption channel is that the bond of the physisorbed species is too weak to survive for a sufficiently long time to reach the detector. IP values of lead and acetone are 7.42<sup>36</sup> and 9.70<sup>37</sup> eV, respectively. Therefore the positive charge in the heterocluster  $Pb_k(CH_3COCH_3)_n^+$  will reside on lead within the complex, so, even for  $Pb_k(CH_3COCH_3)_n^+$  formed by 'pick-up' of neutral lead clusters by charged acetone clusters, the charge would transfer to the metal.

At least one acetone molecule was adsorbed to all the metal cluster cations observed, and, in the case of  $Pb^+$ , up to six acetone molecules are seen to solvate the metal ion. Stace and coworkers<sup>38</sup> found that up to eight methanol molecules were observed to solvate  $Pb^+$  and  $Pb_2^+$ . This difference between acetone and methanol can be rationalized in terms of the difference of their dipole moments. The dipole moment of acetone is 2.88 D and that of methanol is 1.7 D.<sup>39</sup> The complex with solvent molecules of larger dipole moment would be more stable, so in a qualitative sense fewer acetone molecules may be required to stabilize the metal ion. However, it should be noted that differences between the present experimental apparatus and that of Stace,<sup>38</sup> and also differences in steric effects for the two organic molecules, could also partly account for this difference between acetone and methanol. The same phenomenon was observed<sup>40</sup> in a comparison between methanol and water in their solvation of  $Mg^{2+}$ .

Another trend observed for the association product  $Pb_k(CH_3COCH_3)_n^+$  is that the larger the metal cluster cations, the fewer acetone molecules a single lead cluster cation could adsorb in the initial step. One interpretation of this observation would be that the distribution of positive charge throughout the metal cluster would decrease the effectiveness of any one metal ion to associate with acetone molecules, even though the radius of the metal cluster increased. For a given  $k$  value,  $Pb_k(CH_3COCH_3)_n^+$  generally

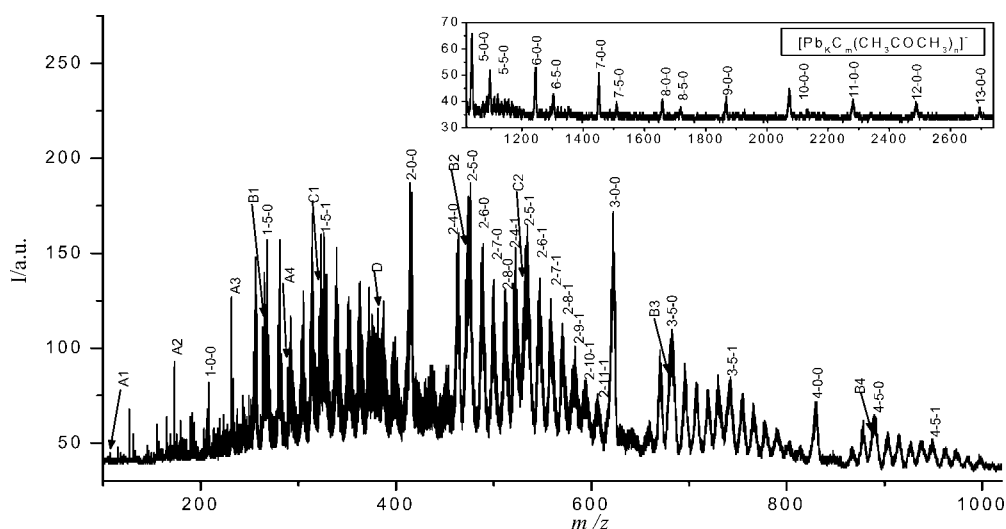
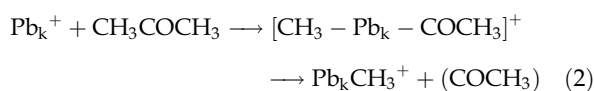


**Figure 3.** Typical TOF mass spectrum for anionic products obtained from the Nd:YAG laser (532 nm, 10 mJ/pulse) irradiation of a lead tablet in the acetone + Ar (95%) mixed carrier gas. The inset (top right) shows the high-mass region. An ( $n = 1-4$ ) denotes  $\text{CH}_2\text{COCH}_3(\text{CH}_3\text{COCH}_3)_n^-$ . Bk ( $k = 1-4$ ) denotes  $\text{Pb}_k(\text{CH}_2\text{COCH}_3)^-$ . Ck ( $k = 1-2$ ) denotes  $\text{Pb}_k\text{CH}_2\text{COCH}_3(\text{CH}_3\text{COCH}_3)^-$ . D denotes  $\text{PbCH}_2\text{COCH}_3(\text{CH}_3\text{COCH}_3)_2^-$ .

had a monotonically decreasing intensity distribution with increasing values of  $n$ , although  $\text{Pb}(\text{CH}_3\text{COCH}_3)_n^+$  exhibited first a monotonically increasing and then decreasing distribution. An obvious precipitous decrease in the intensity of  $\text{Pb}(\text{CH}_3\text{COCH}_3)_5^+$  and  $\text{Pb}_2(\text{CH}_3\text{COCH}_3)_4^+$  was observed; a possible interpretation for this phenomenon was the influence of steric hindrance and a coordination saturation effect, which suggested special structural stability for  $\text{Pb}(\text{CH}_3\text{COCH}_3)_4^+$  and  $\text{Pb}_2(\text{CH}_3\text{COCH}_3)_3^+$ .

#### High-energy pathway $\text{Pb}_k\text{CH}_3^+$

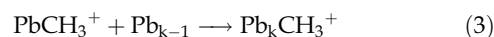
Close to the  $\text{Pb}_k^+$  clusters, peaks at 15 Da higher were observed. These peaks were assigned as  $\text{Pb}_k\text{CH}_3^+$ , and were produced by the dissociative attachment reaction of lead cluster cations  $\text{Pb}_k^+$  with acetone. These peaks did not appear in the blank experiment where only argon was used; in addition, when acetone was replaced by fully deuterated acetone- $d_6$ , peaks at 18 Da higher than  $\text{Pb}_k^+$  were observed, as discussed below. The reaction mechanism of  $\text{Pb}_k^+$  with acetone, observed here, was similar to that of the reaction of  $\text{Cu}^+$  with acetone<sup>10</sup> following the high-energy pathway as shown in reaction (3); one C–C bond of the acetone molecule was cleaved with competitive loss of a neutral fragment.



The preferred ionic product in reaction (2) was  $\text{PbCH}_3^+$ , while the reaction of  $\text{Cu}^+$  with acetone gave  $\text{COCH}_3^+$  as the preferred ionic product.<sup>10</sup> According to Stevenson's rule,<sup>16</sup> the preferred ionic product in reaction (2) is predicted to be the fragment having the lower ionization potential. According to this rule and the experimental result as reported previously,<sup>10</sup>  $\text{IP}(\text{COCH}_3) < \text{IP}(\text{CuCH}_3)$ , and an analogous result  $\text{IP}(\text{PbCH}_3) < \text{IP}(\text{COCH}_3)$  could be deduced here. It

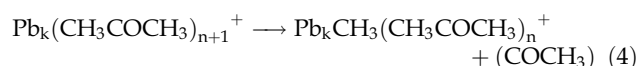
should be noted that the neutral products (in parentheses) of these reactions could not be identified under the present experimental conditions.

If  $\text{Pb}_k\text{CH}_3^+$  was formed via a reaction mechanism as shown in reaction (3), with neutral lead species  $\text{Pb}_x$  participating in the reaction, we should have observed an obvious intensity change of  $\text{Pb}_k\text{CH}_3^+$  as the value of  $k$  increased.



This implies that reaction (3) made a minor or no contribution to the formation of  $\text{Pb}_k\text{CH}_3^+$ , and that oxidative insertion of metal cluster ions as well as of metal atomic ions in organometallic reactions is possible (reaction (2)). The  $\text{CH}_3\text{-COCH}_3$  bond dissociation energy is 80 kcal/mol,<sup>40</sup> but the binding energy of  $\text{Pb}^+\text{-CH}_3$  is not available to our best knowledge. If we assume that the binding energy of  $\text{Pb}^+\text{-CH}_3$  approximately equals the bond dissociation energy of  $\text{CH}_3\text{-Pb}(\text{CH}_3)_3$  ( $49.4 \pm 1$  kcal/mol<sup>41</sup>), then the ground-state reaction for  $\text{Pb}^+$  in reaction (2) is endothermic by about 30 kcal/mol.

An intraheterocluster reaction mechanism was responsible for the formation of  $\text{Pb}_k\text{CH}_3(\text{CH}_3\text{COCH}_3)_n^+$ , as shown in reaction (4), which was proposed for the formation mechanism of  $\text{MgOCH}_3(\text{CH}_3\text{OH})_n^+$  from  $\text{Mg}(\text{CH}_3\text{OH})_{n+1}^+$  and of  $\text{Pb}(\text{CH}_3\text{OH})_n(\text{H}_2\text{O})^+$  from  $\text{Pb}(\text{CH}_3\text{OH})_{n+2}^+$  under the same experimental conditions.<sup>30,38</sup>



The intensity distribution of  $\text{Pb}_k\text{CH}_3(\text{CH}_3\text{COCH}_3)_n^+$  with respect to the values of  $n$  was nearly the same as that of  $\text{Pb}_k(\text{CH}_3\text{COCH}_3)_n^+$  when  $k = 1$ . However, when  $k \geq 2$  the abundances of  $\text{Pb}_k\text{CH}_3(\text{CH}_3\text{COCH}_3)_n^+$  were rather small and their distribution with respect to  $n$  was rather even in comparison, with a monotonically decreasing intensity distribution of corresponding  $\text{Pb}_k(\text{CH}_3\text{COCH}_3)_n^+$  species.

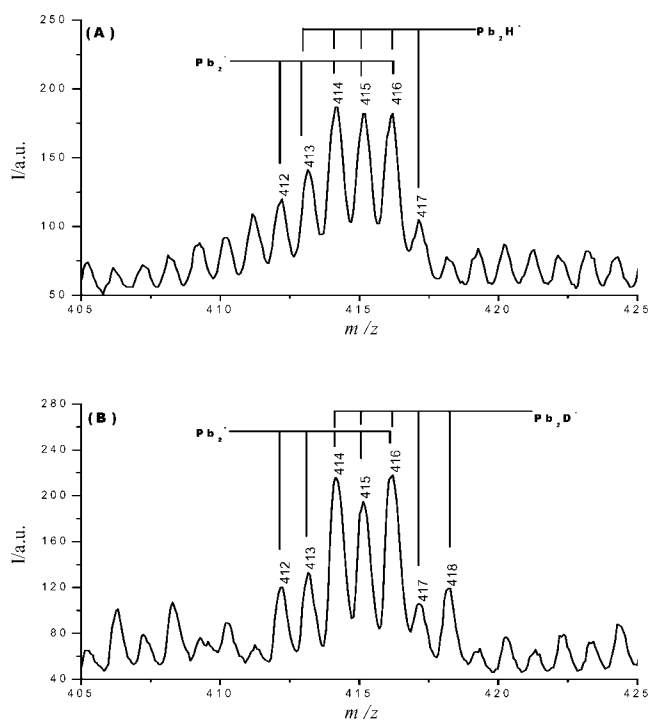


**Figure 4.** (A) Mass scale expansion around  $Pb_2^-$  and  $Pb_2H^-$  to show the isotope pattern and hydrogen resolution resulting from the reaction of lead cluster anions with acetone. (B) Mass scale expansion of  $Pb_2^-$  and  $Pb_2D^-$  to show the isotope pattern and deuterium resolution resulting from the reaction of lead cluster anions with deuterated acetone- $d_6$ .

The overall reduced intensities of  $Pb_kCH_3(CH_3COCH_3)_n^+$  may be subject to three interpretations previously proposed for the same observation in the intraheterocluster reaction of  $Pb(CH_3OH)_{n+2}^+$ , conducted under the same experimental conditions.<sup>38</sup> One interpretation was that  $Pb_k^+$  ( $k \geq 2$ )

experienced greater steric hindrance than  $Pb^+$  in the oxidative insertion reaction. Another explanation was that the distribution of positive charge throughout the metal cluster would decrease the effectiveness of any one metal ion to associate acetone molecules, even though the radius of the metal cluster increased. The third interpretation proposed an increased tendency for metal-metal bond breaking in the larger metal clusters.

### Reaction of lead cluster anions with acetone

Reactions of anionic metal atomic ions (not to mention clusters) have seldom been studied in organometallic reactions. Here we also report our experimental results for the reaction of lead cluster anions with acetone in comparison with that of cations. A typical TOF mass spectrum of the anionic products is shown in Fig. 3. The apparatus had sufficiently high resolution to resolve hydrogen and deuterium atoms coexisting in anionic clusters. Examples of  $Pb_2^-$  with  $Pb_2H^-$  and  $Pb_2^-$  with  $Pb_2D^-$ , formed in the reaction of lead cluster anions with acetone and deuterated acetone- $d_6$  (discussed in the following section), are illustrated in Figs 4(A) and 4(B), respectively.

### $Pb_k^-$ clusters

As for the lead cluster cations  $Pb_k^+$ , lead cluster anions  $Pb_k^-$  are also among the most abundant anionic species observed, with a wide distribution ( $k = 1-13$ ), see Fig. 3. This result also depended on the contribution from the seeded acetone in argon carrier gas, as discussed above for the corresponding cation clusters, since  $Pb_k^-$  could scarcely grow larger than  $Pb^-$  in the corresponding blank experiment in which only pure argon was used. It is noteworthy that  $Pb_7^-$  and  $Pb_{10}^-$  seemed to be 'magic numbers' among the lead cluster anions discussed here. This phenomenon was also observed in the lead cluster anions produced from the reaction of lead cluster anions with deuterated acetone- $d_6$ , as discussed below and shown in Fig. 6.

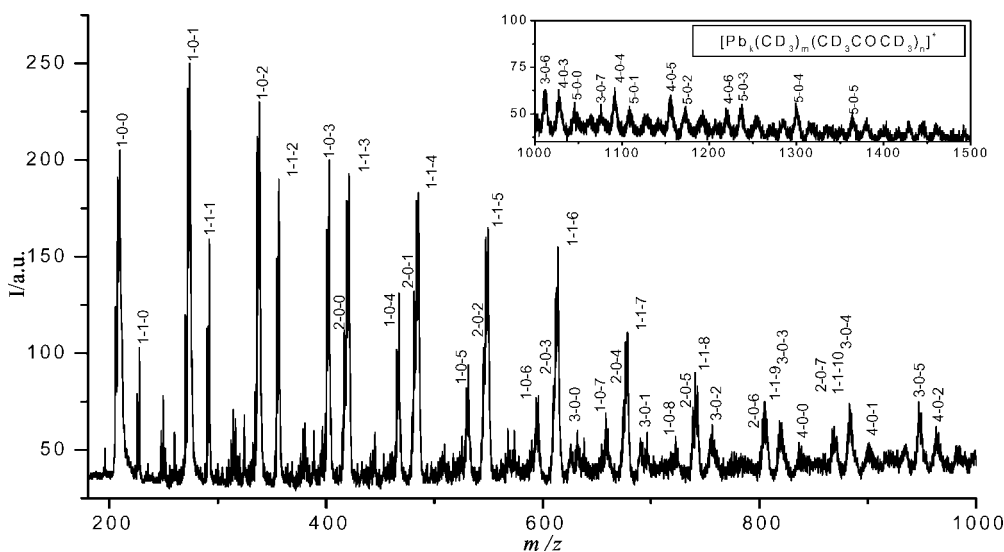


**Figure 5.** Typical TOF mass spectrum for cationic products obtained from the Nd:YAG laser (532 nm, 10 mJ/pulse) irradiation of a lead tablet in the deuterated acetone- $d_6$  + Ar (96.25%) mixed carrier gas. The inset (top right) shows the high-mass region.

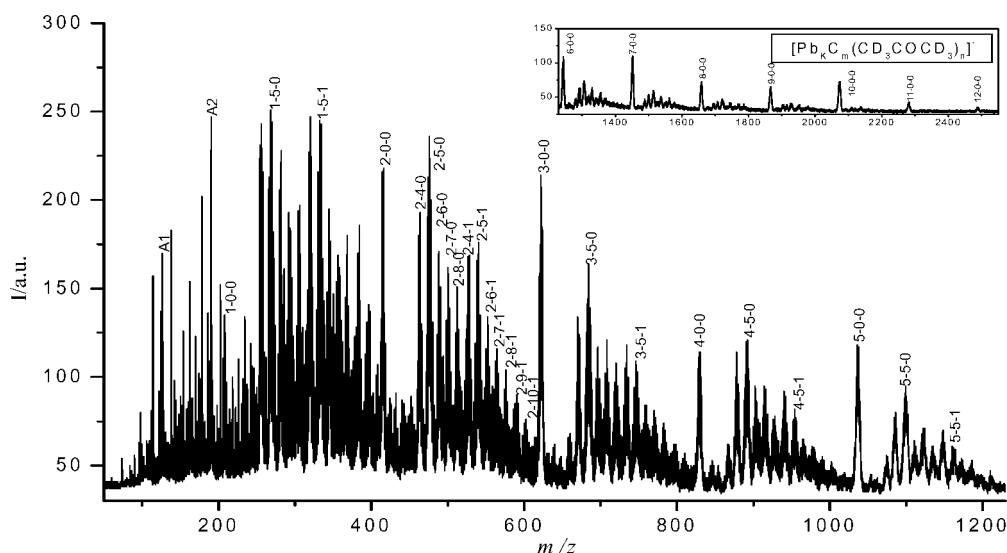


**Figure 6.** Typical TOF mass spectrum for anionic products obtained from the Nd:YAG laser (532 nm, 10 mJ/pulse) irradiation of a lead tablet in the deuterated acetone- $d_6$  + Ar (96.25%) mixed carrier gas. The inset (top right) shows the high-mass region. An  $(n = 1-2)$  denotes  $\text{CD}_2\text{COCD}_3(\text{CD}_3\text{COCD}_3)_n^-$ .

### Metal carbide $\text{Pb}_k\text{C}_m^-$

$\text{Pb}_k\text{C}_m^-$  ( $m = 4-8$ ) clusters, formed from the decomposition of acetone in the plasma, were the predominant anionic products, as shown in Fig. 3. When  $m \leq 3$ ,  $\text{Pb}_k\text{C}_m^-$  clusters could scarcely be observed or distinguished, indicating that these clusters either are unstable or are difficult to form under the present experimental conditions.

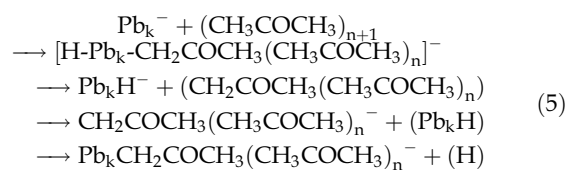
The acetone decomposition processes might include dehydration, dehydrogenation, etc. The underlying mechanism for this decomposition process is presumably determined by the thermodynamics involved. The cluster formation and the following decomposition process and carbide formation were all exothermic. Also, in the experiment, the cluster was 'heated', which promoted the formation of small molecules containing hydrogen and (or) oxygen atoms and their 'evaporation' from the cluster.<sup>42-44</sup> Mixed metal-carbon clusters  $\text{Pb}_k\text{C}_m^-$  grew as the plasma was quenched by collisions with excess expansion gas argon.

For a given  $k$  value,  $\text{Pb}_k\text{C}_m^-$  had first a monotonically increasing and then monotonically decreasing intensity distribution, with a 'magic number' at  $m = 5$ , which was also observed in Fig. 6 (discussed below) and suggested special structural stability for  $\text{Pb}_k\text{C}_5^-$ . This intensity distribution did not change with the variation of  $k$ , indicating that the formation and structure of the  $\text{C}_m$  moiety in  $\text{Pb}_k\text{C}_m^-$  played a predominant role in the formation and structure of these species. Due to the low abundances of the corresponding precursor bare lead cluster anions, this distribution could not be easily observed for  $k \geq 6$ . The  $\text{C}_m$  moiety here should interact with the  $\text{Pb}_k$  cluster as a whole. Size-selected ultraviolet photoelectron spectrometry (UPS) studies of  $\text{C}_m^-$  had shown that  $\text{C}_m^-$  ions appeared to have linear chain structures when  $m < 10$ .<sup>45</sup>

$\text{Pb}_k\text{C}_m^-$  could undergo further association reaction with acetone to give  $\text{Pb}_k\text{C}_m(\text{CH}_3\text{COCH}_3)^-$  ( $m = 4-11$ ), see Fig. 3. It is interesting to note that only one acetone molecule was

adsorbed here. The intensity distribution of  $\text{Pb}_k\text{C}_m^-$  ( $\text{CH}_3\text{COCH}_3$ ) $^-$  was the same as that of  $\text{Pb}_k\text{C}_m^-$ .  $\text{Pb}_k^-$ ,  $\text{Pb}_k\text{C}_m^-$ , and  $\text{Pb}_k\text{C}_m(\text{CH}_3\text{COCH}_3)^-$  all had corresponding hydrogen-containing clusters:  $\text{PbH}^-$ ,  $\text{PbC}_m\text{H}^-$ , and  $\text{Pb}_k\text{C}_m\text{H}^-$  ( $\text{CH}_3\text{COCH}_3$ ) $^-$ , respectively. No detailed discussion of these is given here.

Besides the above-mentioned anionic products,  $\text{Pb}_k\text{H}^-$ ,  $\text{CH}_2\text{COCH}_3(\text{CH}_3\text{COCH}_3)_n^-$  ( $n = 1-4$ , denoted as An in Fig. 3),  $\text{Pb}_k\text{CH}_2\text{COCH}_3^-$  ( $k = 1-4$ , denoted as Bk in Fig. 3),  $\text{Pb}_k(\text{CH}_2\text{COCH}_3)(\text{CH}_3\text{COCH}_3)^-$  ( $k = 1-2$ , denoted as Ck in Fig. 3), and  $\text{Pb}(\text{CH}_2\text{COCH}_3)(\text{CH}_3\text{COCH}_3)_2^-$  (denoted as D in Fig. 3) were observed. The underlying mechanism for their formation requires further experiments. Oxidative insertion of the metal anions  $\text{Pb}_k^-$  into one C-H bond of an acetone molecule, followed by selective simple bond cleavage as proposed in reaction (5), is possible.



### Reactions of lead cluster cations and anions with deuterated acetone- $d_6$

To investigate the isotope effect for the reactions described above and to verify our previous structural assignments of the reaction products, reactions of lead cluster cations and anions with deuterated acetone- $d_6$  were also conducted. Typical TOF mass spectra for cationic and anionic products are shown in Figs 5 and 6, respectively. As can be seen from Figs 5 and 6 in comparison with Figs 2 and 3, respectively, nearly all corresponding deuterated products with the same relative intensity distributions were observed. This confirmed our interpretations in Figs 2 and 3, and to some extent

verified the reaction mechanisms proposed for the reactions of lead cluster cations and anions with acetone. It is noteworthy that the series of clusters  $\text{Pb}_k\text{CD}_2\text{COCD}_3\text{-(CD}_3\text{COCD}_3)_n^-$ , formed in the reaction of lead cluster anions with deuterated acetone- $d_6$  and corresponding to Bk, Ck, and D shown in Fig. 3, were difficult to distinguish in Fig. 6 since these clusters overlapped with the adjacent clusters.

Only the significant differences arising from the deuterium substitution are discussed below. The stronger hydrogen bonds formed by deuterium substitution in the cluster system resulted in larger solvated clusters. For example, in the case of  $\text{Pb}^+$ , up to eight acetone- $d_6$  molecules could be adsorbed, while the corresponding number for acetone was six; in addition,  $\text{PbCD}_3(\text{CD}_3\text{COCD}_3)_n^+$  could grow as large as  $\text{PbCD}_3(\text{CD}_3\text{COCD}_3)_{10}^+$  in comparison with  $\text{PbCH}_3(\text{CH}_3\text{COCH}_3)_6^+$  for acetone.  $\text{Pb}_7^-$  and  $\text{Pb}_{10}^-$  can easily be seen as 'magic numbers' in Fig. 6.

## CONCLUSIONS

Besides chemisorption of acetone on lead cluster ions, high-energy pathway reactions also occurred between lead cluster ions and acetone. Lead cluster cations can undergo oxidative insertion into the carbon-carbon bond in the acetone molecule.  $\text{Pb}_k^+$  ( $k = 1-10$ ),  $\text{Pb}_k(\text{CH}_3\text{COCH}_3)_n^+$  ( $k = 1-8$ ;  $n = 1-6$ ),  $\text{Pb}_k\text{CH}_3^+$  ( $k = 1-5$ ),  $\text{Pb}_k\text{CH}_3(\text{CH}_3\text{COCH}_3)_n^+$  ( $k = 1-4$ ;  $n = 1-6$ ) were the main cationic ion products. The main anionic products were  $\text{Pb}_k\text{C}_m^-$  ( $k = 1-4$ ;  $m = 4-11$ ),  $\text{Pb}_k\text{C}_m(\text{CH}_3\text{COCH}_3)^-$  ( $k = 1-4$ ;  $m = 3-8$ ),  $\text{CH}_2\text{COCH}_3\text{-(CH}_3\text{COCH}_3)_n^-$  ( $n = 1-4$ ), and  $\text{Pb}_k\text{CH}_2\text{COCH}_3(\text{CH}_3\text{COCH}_3)_n^-$  ( $k = 1-4$ ;  $n = 0-2$ ). Special structures and stabilities of the  $\text{C}_m$  moiety played a dominant role in the formation of  $\text{Pb}_k\text{C}_m^-$  clusters.

## Acknowledgements

The authors gratefully acknowledge the support of the National Natural Science Foundation of China under Grant 29890211. We are indebted to Professor Qihe Zhu and Zhen Gao for their original design and assembly of the experimental apparatus. We are also indebted to Professor Hongfei Wang and Fanao Kong for their helpful discussions.

## REFERENCES

1. Tzeng WB, Wei S, Castleman AW Jr. *J. Am. Chem. Soc.* 1989; **111**: 6035.
2. Munson MSB. *J. Am. Chem. Soc.* 1965; **87**: 5313.
3. Blair AS, Harrison AG. *Can. J. Chem.* 1973; **15**: 703.
4. Luczynski Z, Wincel H. *Int. J. Mass Spectrom. Ion Phys.* 1977; **23**: 37.
5. Sieck LW, Ausloos P. *P. Radiat. Res.* 1972; **52**: 47.
6. MacNeil KAG, Futrell JH. *J. Phys. Chem.* 1972; **76**: 409.

7. Weiheimer CJ, Lisy JM. *Chem. Phys.* 1998; **239**: 357.
8. Selegue TJ, Cabarcos OM, Lisy JM. *J. Chem. Phys.* 1994; **100**: 4790.
9. Larsen BS, Ridge DP. *J. Am. Chem. Soc.* 1984; **106**: 1912.
10. Burnier RC, Byrd GD, Freiser BS. *Anal. Chem.* 1980; **52**: 1641.
11. Hanratty MA, Beauchamp JL, Illies AJ, Bowers MT. *J. Am. Chem. Soc.* 1988; **110**: 1.
12. Remick RJ, Asunta TA, Skell PS. *J. Am. Chem. Soc.* 1979; **101**: 1320.
13. Allison J, Freas RB, Ridge DP. *J. Am. Chem. Soc.* 1979; **101**: 1332.
14. Halle LF, Crowe WE, Armentrout PB, Beauchamp JL. *Organometallics* 1984; **3**: 1694.
15. Robinson PJ, Holbrook KA. *Unimolecular Reactions*, Wiley Interscience: New York, 1972.
16. Stevenson DP. *Discuss. Faraday Soc.* 1951; **10**: 35.
17. Tolbert MA, Beauchamp JL. *J. Am. Chem. Soc.* 1984; **106**: 8117.
18. Allison J, Ridge DP. *J. Am. Chem. Soc.* 1978; **100**: 163.
19. Schilling JB, Beauchamp JL. *J. Am. Chem. Soc.* 1988; **110**: 15.
20. Aylett BJ. *Organometallic Compounds 1. The Main Group Elements: Groups IV and V*. Chapman and Hall: London, 1956.
21. Greninger D, Kollonitsch V, Kline CH. *Lead Chemicals*. ILZRO, 1977.
22. Elschenbroich CH, Salzer A. *Organometallics: A Concise Introduction*. VCH: Weinheim, 1992.
23. Guo BC, Purnell JW, Castleman AW Jr. *Chem. Phys. Lett.* 1990; **168**: 155.
24. Venkatachalapathy R, Davila GP, Prakash J. *Electrochem. Commun.* 1999; **1**: 614.
25. Barran PE, Mikhailov V, Stace AJ. *J. Phys. Chem. A* 1999; **103**: 8792.
26. Tian ZX, Xing XP, Tang ZC. *Rapid Commun. Mass Spectrom.* 2002; **16**: 1515.
27. Beig G, Brasseur G. *Geophys. Res. Lett.* 1999; **26**: 1303.
28. Dewar MJS. *Bull. Soc. Chim. Fr.* 1951; **18**: C79.
29. Chatt J, Duncanson LA. *J. Chem. Soc.* 1953; 2939.
30. Lu WY, Yang SH. *J. Phys. Chem. A* 1998; **102**: 825.
31. Hirsch C, Lacor C, Dener C, Vucinic D. *AGARD-CP-510*, 1992.
32. Muhlbach J, Pfau P, Sattler K, Recknagei E. *Z. Phys. B* 1982; **47**: 233.
33. Phillips JC. *J. Chem. Phys.* 1987; **87**: 1712.
34. Clemmer DE, Chen YM, Khan FA, Armentrout PB. *J. Phys. Chem.* 1994; **98**: 6522.
35. Lu WY, Huang RB, Yang SH. *J. Phys. Chem.* 1995; **99**: 12099.
36. Suzer S, Banna MS, Shirley DA. *J. Chem. Phys.* 1975; **63**: 3473.
37. Traeger JC, McLoughlin RG, Nicholson AJC. *J. Am. Chem. Soc.* 1982; **104**: 5318.
38. Barran PE, Mikhailov V, Stace AJ. *J. Phys. Chem. A* 1999; **103**: 8792.
39. Lide DR (ed). *CRC Handbook of Chemistry and Physics* (77th edn). CRC Press: London, 1996.
40. Cox JD, Pilcher G. *Thermochemistry of Organic and Organometallic Compounds*, Academic Press: London, 1970.
41. Gilroy KM, Price SJ, Webster NJ. *Can. J. Chem.* 1972; **50**: 2639.
42. Berg C, Schindler T, Kantlehner M, Schatterburg GN, Bondybey V. *Chem. Phys.* 2000; **262**: 143.
43. Albeit G, Berg C, Beyer M, Achatz U, Joos S. *Chem. Phys. Lett.* 1997; **268**: 235.
44. Bondybey VE, Beyer M, Achatz U, Fox B, Niedner-Schatteburg G. In *Metal Ion Solvation and Metal-Ligand Interactions*, vol. 5. Duncan MA (ed). JAI Press: Stamford, Connecticut, 2000.
45. Yang S, Taylor KJ, Crayraft MJ, Conceicao J, Pettiette CL, Cheshnovsky O, Smalley RE. *Chem. Phys. Lett.* 1988; **144**: 431.